Journal of Materials Chemistry A

RSC Publishing

PAPER

View Article Online
View Journal | View Issue

Cite this: J. Mater. Chem. A, 2013, 1, 4693

The synthesis of porous materials with macroscopically oriented mesopores interconnected by branched mesopores†

Xuemei Sun, Zhitao Zhang, Guozhen Guan, Longbin Qiu and Huisheng Peng*

Received 15th December 2012
Accepted 4th February 2013

DOI: 10.1039/c3ta00170a

www.rsc.org/MaterialsA

Mesoporous silica has been extensively studied for a wide variety of applications such as transport and storage vehicles of guest materials, where it is critical but remains challenging to control the pore structure at a macroscopic scale. Herein, aligned carbon nanotube (CNT) arrays with thicknesses of up to millimeters have been used as templates to produce macroscopically oriented mesopores in the resulting silica material. The pore size, length, and number density were tuned by varying the diameter, length, and number density of CNTs. When surfactants were co-assembled with the silica precursor, the produced ordered mesopores from the surfactant could further interconnect the macroscopically oriented mesopores. The sizes, densities, and structures of the ordered mesopores have been controlled by varying the surfactants. This interconnected porous structure provided the material with unique advantages, and the use for adsorption of a guest chemical was studied as a demonstration.

Introduction

Mesoporous materials have been widely studied for various promising applications such as separation, catalysis, medicine, and energy storage.[1,2] Among them, mesoporous silica represents one of the most explored systems. Generally, mesoporous silica materials have been synthesized by co-assembling silica precursors and surfactants, followed by the removal of surfactants.[3] The pore sizes were controlled by varying the sizes of the surfactant molecules, which also determined the pore structures, *e.g.*, cetyltrimethylammonium bromide ($C_{16}H_{33}N(CH_3)_3Br$, CTAB) produced hexagonal pores, while both polyoxyethylene (10) cetyl ether ($C_{16}EO_{10}$, Brij56) and poly(ethylene oxide)-*b*-poly(propylene oxide)-*b*-poly(ethylene oxide) ($PEO_{106}PPO_{70}PEO_{106}$, F127) produced cubic pores.[4] Although the pore sizes were dependent on the sizes of surfactant molecules, it was challenging to accurately tune them. For instance, CTAB, Brij56, and F127 were shown to produce mesopores with sizes of ~2 nm, ~3 nm, and ~6 nm, respectively, but pore size ranges of 2–3, 3–6, and larger than 6 nm could not be achieved from them without the assistance of other methods such as the addition of swelling agents.[3] In the case of polymers as surfactants, the mesopore sizes may be tuned by varying the molecular weights of the polymers;[5] however, it was difficult to control the molecular weights of the polymer surfactants in syntheses. In addition, although the mesoporous structures could be highly ordered in local regions by using surfactants as templates, it remained challenging to effectively extend the ordered structure to macroscopic scale. For instance, the hexagonal mesopores derived from CTAB did not penetrate from one side to the other in bulk material, although they appeared to be highly oriented and penetrating in the observed area under microscopy.

To further control the structure, many nanomaterials have been also extensively investigated as templates to produce mesopores. To this end, one-dimensional inorganic nanotubes and nanowires which could be removed by chemical reactions in solutions or under heating have been generally used.[6] Carbon nanotubes (CNTs) represent one of the promising candidates due to the following advantages. CNTs have been easily synthesized on a large scale by a chemical vapor deposition process.[7] The diameters of CNTs could be gradually increased from less than one nanometer for single-walled CNTs to tens of nanometers for multi-walled CNTs by varying the catalyst and other growth conditions, while the lengths of the CNTs could be widely varied from nanometers to millimeters by increasing the growth time.[8] It was easy to further modify the outer surfaces of CNTs with various inorganic and organic molecules, which favored solution fabrication and may incorporate new functionalities.[9] CNTs could be fully removed at relatively low temperatures under heating to produce mesopores, and no complex operations were required. For instance, mesoporous silica was synthesized by hydrolyzing TEOS in the presence of CNTs.[10] However, long CNTs could not be well dispersed in a solution fabrication method, so the resulting mesopores based

State Key Laboratory of Molecular Engineering of Polymers, Department of Macromolecular Science and Laboratory of Advanced Materials, Fudan University, Shanghai 200438, China. E-mail: penghs@fudan.edu.cn

† Electronic supplementary information (ESI) available. See DOI: 10.1039/c3ta00170a

on short CNTs may not be continuous inside. In particular, CNTs were randomly dispersed in composite materials, and it was impossible to obtain oriented or ordered porous structures. Indeed, the resulting mesopores did not penetrate from one side to the other due to the use of short CNTs and the random dispersion of CNTs (Fig. 1a).

Herein, we have discovered a general synthetic strategy for macroscopically oriented mesopores by using aligned CNT arrays as templates. In addition, hierarchical porous materials with macroscopically oriented mesopores interconnected by ordered branched mesopores are realized by the addition of surfactants as a second type of template. The oriented mesopores with lengths up to millimeters penetrated from one side to the other in the silica membrane, while the ordered branched mesopores were located among the macroscopically oriented mesopores. The size and density of oriented mesopores could be accurately controlled by varying the diameter and number density of CNTs, while the size and structure of the ordered branched mesopores may be varied relatively by selecting different surfactants. These novel mesoporous materials have been mainly investigated to adsorb guest chemicals as an application demonstration in this work.

Experimental section

Multi-walled carbon nanotube (MWCNT) arrays were mainly used. The detailed synthesis of the aligned MWCNT arrays has been previously reported,[11,12] and it is further summarized in the ESI.† The mesoporous silica with only macroscopically oriented and penetrating cylindrical mesopores was synthesized by two main steps. Firstly, MWCNT arrays were immersed in a solution mixture of 2.08 g TEOS, 5.5 g EtOH, 0.5 g deionized water and 0.4 g (0.1 M) HCl for 12 h at 70 °C and then dried at room temperature. To obtain high quality composite arrays, the solution mixture was previously stirred for 1 h to produce the pre-polymeric silica sol. Secondly, aligned MWCNTs were removed to produce the mesoporous silica after calcination in air at 750 °C for 2 h (heating rate of 5 °C min^{-1}). To introduce the second interconnected mesopores, surfactants such as CTAB ($C_{16}H_{33}N(CH_3)_3Br$), Brij56 ($C_{16}EO_{10}$) and F127 ($EO_{106}PO_{70}EO_{106}$) were added to the mixed solution with molar ratios between surfactant and TEOS of 0.10 : 1, 0.08 : 1 and 0.005 : 1, respectively. The surfactant phase was also removed during the calcination in the second step. The silica–MWCNT composite arrays appeared black due to the MWCNTs. After removal of the MWCNTs, the resulting mesoporous silica was colorless.

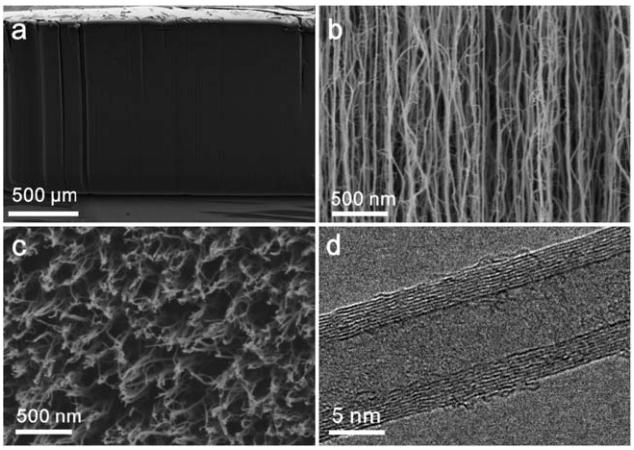

Fig. 2 (a)–(c) Scanning electron microscopy (SEM) images of a bare MWCNT array in side view at different magnifications, and top view, respectively. (d) Transmission electron microscopy (TEM) image of an MWCNT.

For the adsorption measurements, about 40 mg of different mesoporous materials were immersed in 4 mL of rhodamine 6G (R6G)/H_2O solution (concentration of 10 μg mL^{-1}) for 12 h. The adsorbed amount of R6G in the mesoporous material was calculated by comparing the R6G solution before and after adsorption based on the difference in R6G absorption intensities in the UV-vis spectra. A standard curve of concentration and absorption intensity was used for the calculation.

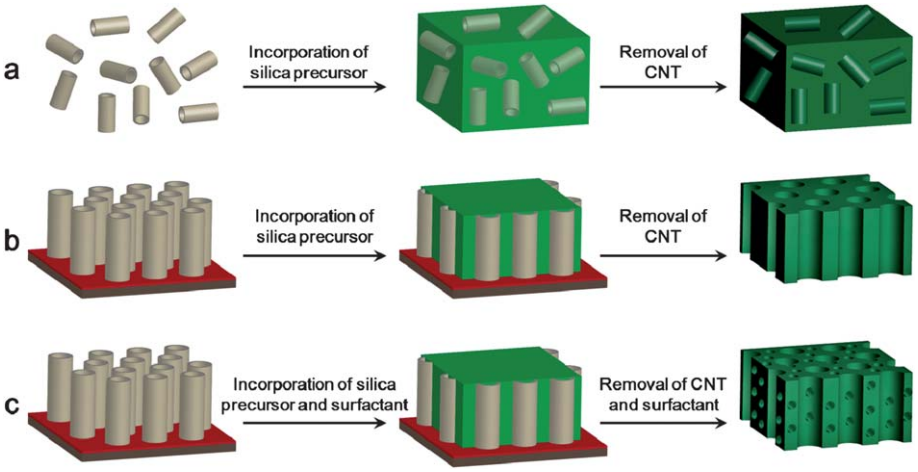

Fig. 1 Schematic illustration of the synthesis of mesoporous silica materials. (a) The conversional synthesis of mesopores with a disordered structure based on randomly dispersed CNTs as templates. (b) The preparation of macroscopically oriented mesopores from the aligned CNT array template. (c) The formation of macroscopically oriented mesopores which are interconnected by branched mesopores using the aligned CNT array and surfactant as templates.

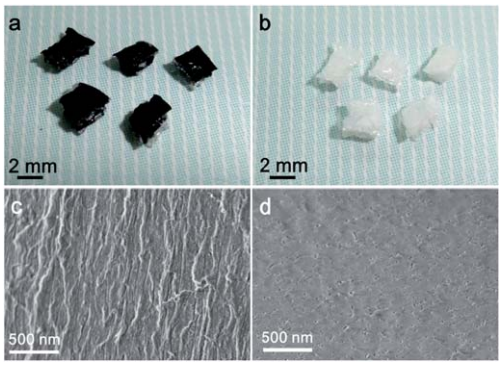

Fig. 3 (a) Photograph of an MWCNT–silica composite array. (b) Photograph of a mesoporous silica array after removal of MWCNTs in (a). (c) and (d) SEM images of the resulting mesoporous silica in side and top views, respectively.

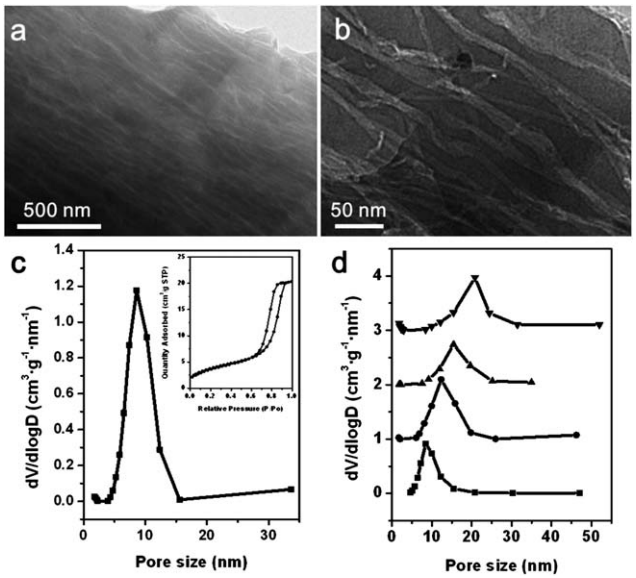

Fig. 4 (a) and (b) TEM images of the resulting mesoporous silica with different magnifications. (c) Pore size distribution and nitrogen sorption isotherms (inset) for (a). (d) Pore size distributions of a series of mesoporous silica arrays with increasing pore sizes.

Structures were characterized by scanning electron microscopy (SEM, Hitachi FE-SEM S-4800, operated at 1 kV) and transmission electron microscopy (TEM, JEOL JEM -2100F, operated at 200 kV). For TEM measurements, the samples were prepared by grinding the materials into powder and dispersing them in ethanol, followed by dropping the mixture onto copper grids and evaporating off ethanol at room temperature. Nitrogen sorption isotherms were performed on a Micromeritics ASAP 2020 analyzer at 77 K. The samples were degassed at 500 °C for 6 h prior to the measurements. The pore size distribution was derived from the adsorption branch using the Barrett–Joyner–Halenda (BJH) model. Small-angle X-ray scattering (SAXS) patterns were produced from a Nanostar U SAXS system (Bruker, Cu Kα radiation). The porous silica materials were attached to the sample holder with oriented mesopores perpendicular to the path of the incident X-rays. Two-dimensional SAXS patterns were directly obtained, while linear patterns were generated by a full integration of diffraction dots. The UV-vis spectra were obtained from a SHIMADZU UV-3150.

Results and discussion

Although a wide variety of mesoporous materials could be synthesized by using the aligned CNT array and surfactant as hard and soft templates, respectively, here, mesoporous silica was mainly studied as a demonstration of such a novel structure. The synthetic details were schematically shown in Fig. 1b and c. Briefly, aligned CNT arrays were firstly grown from an iron catalyst by chemical vapor deposition (Fig. S1†), followed by incorporation of a silica precursor without or with surfactants. The surfactant would be co-assembled among the aligned CNTs in the latter case. The CNTs maintained their highly aligned structure during the infiltration process. The precursors underwent hydrolysis and condensation reactions to produce silica. Both CNTs and surfactant were finally removed to generate mesopores after calcination.

Multi-walled carbon nanotube (MWCNT) arrays were mainly used in this work due to their easy synthesis and structural control. Fig. 2a shows a scanning electron microscopy (SEM) image of a typical array with a thickness of ~1 mm. Fig. 2b and c further show the side and top views, respectively, at higher magnifications. The MWCNTs are highly aligned and perpendicular to the substrate. Fig. 2d further shows a transmission electron microscopy (TEM) image of a typical MWCNT with a diameter of ~10 nm. No obvious impurities have been found on the surface of the MWCNTs. The diameters of the MWCNTs were controlled to be from 7 to 30 nm mainly by varying the catalyst thickness.[13,14] The array thicknesses could be easily controlled typically from hundreds of micrometers to several millimeters by increasing the growth time.[13] For instance, arrays with thicknesses of 400 μm and 1 mm were synthesized after 12 and 30 min, respectively. The MWCNT arrays with a thickness of ~1 mm were mainly used.

Fig. 2b and c also showed that there were a lot of voids among neighboring MWCNTs, and the void sizes were tuned by varying the number density of MWCNTs with the same diameter. For an average diameter of 10 nm, the number density of MWCNTs was changed from 10^{10} to 10^{12} cm^{-2}, which produced a void size of tens to hundreds of nanometers.[15,16] Therefore, the second phase can be effectively infiltrated into the array through a solution process.[12,16,17] Tetraethyl orthosilicate (TEOS), a widely used precursor for silica materials,[18] was incorporated to produce CNT–silica composite arrays. Both the array sizes and morphologies were not obviously changed after the solution incorporation. In other words, the MWCNT structure should be well maintained in the resulting composite arrays. Fig. S2† further showed typical SEM images of such a composite array in side and top views. As expected, the voids among the MWCNTs were fully filled by the silica precursor. In addition, the MWCNTs maintained a highly aligned structure in the composite array.

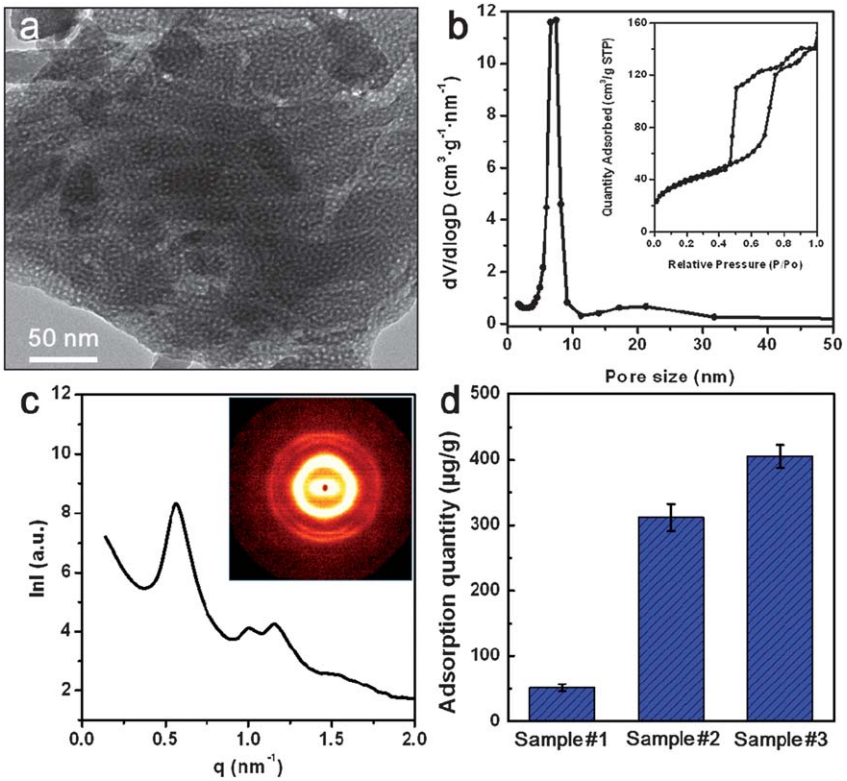

Fig. 5 The resulting mesoporous silica derived from aligned MWCNTs and F127 as templates to produce trunk and branched mesopores, respectively. (a) TEM image. (b) Size distributions of the two mesopores. (c) SAXS pattern. (d) Comparison of the adsorption capacity by using R6G as a model. Samples #1, #2, and #3 correspond to mesoporous silica materials derived only from aligned MWCNTs, only from F127, and from both aligned MWCNTs and F127, respectively.

The MWCNTs were then removed to produce silica materials with macroscopically penetrating mesopores by calcination at a temperature higher than 700 °C in air (Fig. 1b). The MWCNT–silica composite arrays appeared black which arose from the MWCNTs, while the resulting silica was colorless after removal of the MWCNTs (Fig. 3a and b). Therefore, this allowed us to conveniently monitor the calcination process with the naked eye. It should be noted that the array sizes and morphologies remained almost unchanged after the removal of MWCNTs. In other words, these materials were mechanically stable with high structural integrity. Fig. 3c and d showed SEM images of the mesoporous silica in side and top views, respectively. The number density of $\sim 10^{11}$ cm^{-2} of cylindrical mesopores was the same as that of the original MWCNTs. In addition, oriented long mesopores and open ends with a diameter of about 11 nm, similar to the MWCNT diameter, can be clearly observed. The oriented structure of the cylindrical mesopores was also confirmed by two-dimensional small angle X-ray scattering (SAXS). Two intense diffraction spots in bilateral symmetry clearly indicated the alignment of mesopores.[19] In strong contrast, no symmetric spots were observed in the pattern for the mesoporous silica which was synthesized by using a randomly dispersed MWCNT material as a template under the same conditions (Fig. S3†).

The cylindrical mesopores in the silica were further verified by TEM (Fig. 4a and b). Nitrogen sorption isotherms showed typical hysteresis loops which were close to H1 type (inset image in Fig. 4c)[20] and a capillary condensation step in a relative pressure (P/P_0) range of 0.7–0.9, suggesting the formation of cylindrical mesopores with high uniformity.[20,21] The mesopore sizes were calculated to be 8–12 nm from the adsorption data based on the BJH model (Fig. 4c). This size range was consistent with the MWCNTs used. As previously mentioned, the mesopore diameter could be accurately controlled by varying the MWCNT diameter. Fig. 4d showed a series of silica materials with increasing mesopore sizes from 8 to 20 nm.

A mesoporous structure which is limited to local regions has largely hindered applications, *e.g.*, it took a long time for guest molecules to be transported along mesopores in different regions.[22] To this end, the above cylindrical mesopores derived from macroscopically penetrating and aligned MWCNTs show unique advantages for many applications, such as separation membranes, drug-delivery carriers, and chemical catalysts. However, the relatively low surface area may limit their applications. Therefore, surfactants as second templates were further introduced to produce another kind of mesopores which interconnect the macroscopically penetrated and cylindrical mesopores.

A block copolymer of F127 was firstly investigated as a surfactant model to generate the branched mesopores. It was added to the MWCNT array with TEOS during the synthesis. Fig. 5a showed a typical TEM image of the resulting silica materials with two different types of mesopores. The relatively larger trunk mesopores with a size of ~18 nm were derived from

aligned MWCNTs, while the smaller mesopores with a size of ~7 nm as branched mesopores were produced by F127. The sizes of the two mesopores were further shown in Fig. 5b, which was consistent with TEM observations. They were calculated from the adsorption of the nitrogen sorption isotherms with two capillary condensation steps (inset image of Fig. 5b) based on a BJH model. The branched mesopores could be more uniform than the trunk mesopores. The SAXS pattern exhibited three diffraction peaks at 0.57, 1.01, and 1.15 nm^{-1}, which corresponded to *d*-spacing values of 11.04, 6.24, and 5.45 nm, respectively (Fig. 5c).[23,24] They were consistent with mesoporous silica which was synthesized from TEOS and F127 by a traditional method without using MWCNTs (Fig. S4†).[25]

The interconnected mesoporous structure provided a material with unique advantages for various applications. Here, the use for adsorption of a guest chemical, rhodamine 6G (R6G, Fig. S5†), was studied as a demonstration. Fig. 5d compared the adsorption capacities of three different porous materials, *i.e.*, mesoporous silica only derived from aligned MWCNTs (Sample #1), mesoporous silica only derived from F127 (Sample #2), and mesoporous silica derived from both aligned MWCNTs and F127 (Sample #3), under the same conditions (*i.e.*, adsorption time of 12 h). The low adsorption capacity of Sample #1 can be explained by a low pore volume. Obviously, Sample #3 was ~30% higher than Sample #2 due to the fact that the branched mesopores derived from F127 were connected by the trunk mesopores derived from the MWCNTs with more efficient adsorption. As expected, the adsorption rate of Sample #3 was also faster than Sample #2 (Fig. S6†). In addition, according to the measured surface area, although Sample #2 had a larger surface area than both Samples #1 and #3, the adsorbed amounts for Samples #1, #2, and #3 were 3.76 μg m^{-2}, 1.16 μg m^{-2} and 2.81 μg m^{-2}, respectively. In other words, some branched mesopores in Sample #3 had not been effectively interconnected by the trunk mesopores, so the guest molecules could not be rapidly transported to them. More efforts are required to further vary the structures of CNT arrays to optimize these mesoporous materials.

Conclusions

In summary, this work reported a general synthesis of novel porous silica materials with macroscopically oriented trunk mesopores interconnected by highly ordered branched mesopores. The number densities of trunk mesopores were controlled by varying those of the MWCNTs, while their sizes were controlled by varying the diameters of the MWCNTs used. The sizes could be further decreased through the use of single-walled CNTs. The pore sizes of the branched mesopores were controlled by selecting different surfactants. Although F127 was mainly discussed above, other surfactants such as CTAB and Brij56 were also introduced to produce branched mesopores with smaller diameters of ~2.0 and ~2.5 nm, respectively (Fig. S7†). More efforts are also underway to tune the structures of the branched mesopores by the surfactant. The novel mesopore structure was demonstrated to be more efficient for mass transport than the other mesoporous structures, which is critically important for many applications, including catalysis, drug delivery, and energy storage. It should be also noted that, although silica has been mainly shown by this method, other materials such as titanium dioxide and tin dioxide can also be synthesized by this method. Therefore, this work also represents a general route to develop a family of functional porous materials with high performances.

Acknowledgements

This work was supported by NSFC (20904006, 91027025, 21225417), MOST (2011CB932503, 2011DFA51330), STCSM (11520701400, 12nm0503200), Fok Ying Tong Education Foundation and The Program for Professor of Special Appointment at Shanghai Institutions of Higher Learning.

Notes and references

1 F. Li, Z. Wang, N. S. Ergang, C. A. Fyfe and A. Stein, *Langmuir*, 2007, **23**, 3996.
2 Z. Sun, Y. Deng, J. Wei, D. Gu, B. Tu and D. Zhao, *Chem. Mater.*, 2011, **23**, 2176.
3 Y. Wan and D. Zhao, *Chem. Rev.*, 2007, **107**, 2821.
4 D. Zhao, Q. Huo, J. Feng, B. F. Chmelka and G. D. Stucky, *J. Am. Chem. Soc.*, 1998, **120**, 6024.
5 A. C. Finnefrock, R. Ulrich, G. E. S. Toombes, S. M. Gruner and U. Wiesner, *J. Am. Chem. Soc.*, 2003, **125**, 13084.
6 H. Liang, S. Liu and S. Yu, *Adv. Mater.*, 2010, **22**, 3925.
7 V. Bajpai, L. Dai and T. Ohashi, *J. Am. Chem. Soc.*, 2004, **126**, 5070.
8 H. J. Dai, *Acc. Chem. Res.*, 2002, **35**, 1035.
9 V. Georgakilas, A. Bourlinos, D. Gournis, T. Tsoufis, C. Trapalis, A. Mateo-Alonso and M. Prato, *J. Am. Chem. Soc.*, 2008, **130**, 8733.
10 B. C. Satishkumar, A. Govindaraj, E. M. Vogl, L. Basumallick and C. N. R. Rao, *J. Mater. Res.*, 1997, **12**, 604.
11 H. Peng, X. Sun, F. Cai, X. Chen, Y. Zhu, G. Liao, D. Chen, Q. Li, Y. Lu, Y. Zhu and Q. Jia, *Nat. Nanotechnol.*, 2009, **4**, 738.
12 L. Qiu, X. Sun, Z. Yang, W. Guo and H. Peng, *Acta Chimica Sinica*, 2012, **70**, 1523.
13 A. Rizzo, R. Rossi, M. A. Signore, E. Piscopiello, L. Capodieci, R. Pentassuglia, T. Dikonimos and R. Giorgi, *Diamond Relat. Mater.*, 2008, **17**, 1502.
14 K. Liu, Y. Sun, L. Chen, C. Feng, X. Feng, K. Jiang, Y. Zhao and S. Fan, *Nano Lett.*, 2008, **8**, 700.
15 S. Huang, Z. Yang, L. Zhang, R. He, T. Chen, Z. Cai, Y. Luo, H. Lin, H. Cao, X. Zhu and H. Peng, *J. Mater. Chem.*, 2012, **22**, 16833.
16 B. L. Wardle, D. S. Saito, E. J. García, A. J. Hart, R. G. de Villoria and E. A. Verploegen, *Adv. Mater.*, 2008, **20**, 2707.
17 H. Peng and X. Sun, *Chem. Phys. Lett.*, 2009, **471**, 103.
18 D. Zhao, P. Yang, D. I. Margolese and G. D. Stucky, *Chem. Commun.*, 1998, 2499.
19 S. H. Tolbert, A. Firouzi, G. D. Stucky and B. F. Chmelka, *Science*, 1997, **278**, 264.

20 M. Kruk and M. Jaroniec, *Chem. Mater.*, 2001, **13**, 3169.
21 Q. Huo, D. I. Margolese and G. D. Stucky, *Chem. Mater.*, 1996, **8**, 1147.
22 H. Peng, J. Tang, L. Yang, J. Pang, H. S. Ashbaugh, C. J. Brinker, Z. Yang and Y. Lu, *J. Am. Chem. Soc.*, 2006, **128**, 5304.
23 R. Liu, Y. Shi, Y. Wan, Y. Meng, F. Zhang, D. Gu, Z. Chen, B. Tu and D. Zhao, *J. Am. Chem. Soc.*, 2006, **128**, 11652.
24 D. Chen, Z. Li, Y. Wan, X. Tu, Y. Shi, Z. Chen, W. Shen, C. Yu, B. Tu and D. Zhao, *J. Mater. Chem.*, 2006, **16**, 1511.
25 D. Zhao, P. Yang, N. Melosh, J. Feng, B. F. Chmelka and G. D. Stucky, *Adv. Mater.*, 1998, **10**, 1380.